INFECTION AND IMMUNITY, Mar. 2003, p. 1497–1504 Vol. 71, No. 3
0019-9567/03/$08.00+0 DOI: 10.1128/IAI.71.3.1497–1504.2003

Shiga Toxin 1 Triggers a Ribotoxic Stress Response Leading to p38 and JNK Activation and Induction of Apoptosis in Intestinal Epithelial Cells

Wendy E. Smith,[1] Anne V. Kane,[1] Sausan T. Campbell,[1] David W. K. Acheson,[2] Brent H. Cochran,[3] and Cheleste M. Thorpe[1]*

Division of Geographic Medicine and Infectious Diseases, Department of Medicine, Tufts—New England Medical Center,[1] and Department of Physiology, Tufts University School of Medicine,[3] Boston, Massachusetts, and Center for Food Safety and Applied Nutrition, Food and Drug Administration, College Park, Maryland[2]

Received 11 September 2002/Accepted 25 November 2002

Shiga toxins made by Shiga toxin-producing *Escherichia coli* (STEC) are associated with hemolytic uremic syndrome. Shiga toxins (Stxs) may access the host systemic circulation by absorption across the intestinal epithelium. The effects of Stxs on this cell layer are not completely understood, although animal models of STEC infection suggest that, in the gut, Stxs may participate in both immune activation and apoptosis. Stxs have one enzymatically active A subunit associated with five identical B subunits. The A subunit inactivates ribosomes by cleaving a specific adenine from the 28S rRNA. We have previously shown that Stxs can induce multiple C-X-C chemokines in intestinal epithelial cells in vitro, including interleukin-8 (IL-8), and that Stx-induced IL-8 expression is linked to induction of c-Jun mRNA and p38 mitogen-activated protein (MAP) kinase pathway activity. We now report Stx1 induction of both primary response genes *c-jun* and c-*fos* and activation of the stress-activated protein kinases, JNK/SAPK and p38, in the intestinal epithelial cell line HCT-8. By 1 h of exposure to Stx1, mRNAs for *c-jun* and c-*fos* are induced, and both JNK and p38 are activated; activation of both kinases persisted up to 24 h. Stx1 enzymatic activity was required for kinase activation; a catalytically defective mutant toxin did not activate either. Stx1 treatment of HCT-8 cells resulted in cell death that was associated with caspase 3 cleavage and internucleosomal DNA fragmentation; this cytotoxicity also required Stx1 enzymatic activity. Blocking Stx1-induced p38 and JNK activation with the inhibitor SB202190 prevented cell death and diminished Stx1-associated caspase 3 cleavage. In summary, these data link the Stx1-induced ribotoxic stress response with both chemokine expression and apoptosis in the intestinal epithelial cell line HCT-8 and suggest that blocking host cell MAP kinases may prevent these Stx-associated events.

Shiga toxin-producing *Escherichia coli* (STEC) is an important cause of morbidity and mortality in the United States (2). Approximately 5 to 10% of individuals infected with STEC will develop serious complications, such as hemorrhagic colitis and hemolytic-uremic syndrome (HUS) (23). However, our understanding of exactly how and where Shiga toxins exert their pathogenic effects in the human host is not complete.

Because STEC is a noninvasive intestinal pathogen, it has been proposed that Shiga toxins produced by bacteria in the host intestinal lumen must cross the intestinal epithelium in order to cause disease in distal organs. The extent to which Shiga toxins are absorbed systemically may influence who is at risk for the serious complications of STEC infection. In vitro, inflammation of intestinal epithelium can affect permeability and hence uptake of substances present near the apical surface of the intestinal epithelial cell monolayer (21, 22). Hurley, Thorpe, and Acheson have hypothesized that intestinal inflammation may affect how much Shiga toxin is absorbed (13). In one early clinical study, severity of colitis was linked to development of HUS (10). Using an in vitro model of polarized intestinal epithelium, Hurley et al. showed that neutrophil transmigration enhances Shiga toxin absorption across intestinal epithelium (13).

Shiga toxins have been classically appreciated as ribosome intoxicating proteins, exerting their effects on cells by blocking new protein synthesis. It was long thought that Shiga toxin's role in HUS pathogenesis was as a cytotoxin, causing cell death by preventing synthesis of critical host proteins needed by the cell to survive and/or function properly. However, as a result of intense investigation of Shiga toxin's effects on the different host cell types thought to be important targets in HUS pathogenesis, it has recently been appreciated that Shiga toxins can stimulate significant cytokine release from many cell types (reviewed in reference 11), reinforcing the hypothesis that Shiga toxin-induced host cell immune activation in the gut may play an important role in the development of HUS following infection with STEC. The intestinal epithelium is the first host tissue in contact with Shiga toxins, and it is possible that the initial Shiga toxin-intestinal epithelial cell interaction may be central to this immune activation. Our laboratory has focused on understanding the Shiga toxin-intestinal epithelium interaction. We have demonstrated that Shiga toxin-induced C-X-C chemokine expression in intestinal epithelial cells, occurring at

* Corresponding author. Mailing address: Division of Geographic Medicine and Infectious Diseases, New England Medical Center, 750 Washington St., Box 041, Boston, MA 02111. Phone: (617) 636-0245. Fax: (617) 636-5292. E-mail: cthorpe@lifespan.org.

least in part via enhanced chemokine mRNA stability, is paradoxically correlated with the degree of protein synthesis inhibition (25, 26).

We also observed that Shiga toxin-induced interleukin-8 (IL-8) protein expression from intestinal epithelial cells could be diminished by specifically inhibiting the p38 mitogen-activated protein (MAP) kinase pathway (25). MAP kinases can be divided into two basic groups (19). Classically, extracellular regulated kinases 1 and 2 (ERKs 1 and 2) are stimulated by mitogens and are involved in cell growth and differentiation. In contrast, the stress-activated protein kinases, Jun N-terminal kinases (SAPKs/JNKs), and p38 MAP kinases are stimulated by cellular stress, such as osmotic shock or UV irradiation, or by proinflammatory cytokines. In 1997, Iordanov et al. made an important observation about the SAPK/JNKs and protein synthesis inhibitors, demonstrating that two protein synthesis inhibitors that specifically damaged the 28S rRNA resulted in altered host signal transduction, including induction of the primary response genes c-*fos* and *c-jun* and activation of JNKs (15). These protein synthesis inhibitors were anisomycin and ricin. Iordanov and colleagues termed this response ribotoxic stress. Although anisomycin has a distinct footprinting site on the 28S rRNA, the A-subunit of ricin has the same *N*-glycosidase activity as the A-subunit of Shiga toxins, acting on the α-sarcin loop.

Recently, several authors have implicated MAP kinase activation in Shiga toxin-induced tumor necrosis factor alpha (TNF-α) expression in various target cell lines other than intestinal epithelium (9, 20). Nakamura and colleagues have shown that in renal tubular epithelial cells, Shiga toxin 2 (Stx2) activates p38 and that Stx2-induced TNF-α expression is diminished by blocking the p38 pathway. Foster et al. have shown that p38 and JNK are activated by Stx1 in a mononuclear cell line and that blocking p38 diminished Stx1-induced TNF-α expression. In addition, Stx1-induced p38 activation has been associated with cytotoxicity. In Vero cells, an inhibitor of the p38 pathway blocked Stx1-induced cytotoxicity, thereby linking p38 activation to Vero cell death (14).

Shiga toxins have also been linked with cellular apoptosis in the intestine in studies both in vitro and in vivo. Studies from Barnett-Foster et al. and Jones et al. demonstrated that Shiga toxins may play a role in inducing apoptosis in some intestinal epithelial cell lines (3, 17). Shiga toxins have previously been observed to mediate intestinal damage by cellular apoptosis in a rabbit ileal loop model (18).

Based on these data and our previous observations, we hypothesized that Shiga toxins could induce both p38 and JNK activation in intestinal epithelial cells through a ribotoxic stress mechanism, based on *N*-glycosidase activity, and that Shiga toxin-induced cytotoxicity resulted primarily from this MAP kinase activation. Since intestinal epithelial cells are the critical primary target in the toxin's eventual dissemination to distal organs, the purpose of this study was to identify the signal transduction events that precede Shiga toxin-associated chemokine expression and cytotoxicity in HCT-8 cells. We compare the effects on p38 and JNK of Stx1 and a mutant Stx1 with a substitution in the active site. We examine the duration of Stx1-induced p38 and JNK activation in intestinal epithelial cells, the mechanism by which Stx1 induces cell death and, finally, the effects of inhibition of p38 and JNK on Stx1-induced apoptosis. These studies are novel because we demonstrate the link between *N*-glycosidase activity, Stx1-induced p38 and/or JNK activation, and Stx1-induced apoptosis.

MATERIALS AND METHODS

Cell culture, materials, and solutions. HCT-8 cells were obtained from the American Type Culture Collection and cultured at 37°C in 5% CO_2 in RPMI 1640 medium with L-glutamine, 10% fetal calf serum, 100 U of penicillin G sodium per ml, 100 μg of streptomycin sulfate per ml, 1 mM sodium pyruvate, and 10 mM HEPES, as previously described (25). Cell culture media and additives were obtained from GibcoBRL-Life Technologies (Grand Island, N.Y.). Qiashredder cell homogenization spin columns and RNeasy kits were obtained from Qiagen, Inc. (Santa Clarita, Calif.). Northern blotting glyoxal gel preparation and transfer reagents and nylon membranes were obtained from Ambion, Inc. (Austin, Tex.). [^{3}H]leucine and [α-^{32}P]dCTP were obtained from New England Nuclear (Boston, Mass.). Bio-Rad protein assay reagent was obtained from Bio-Rad (Hercules, Calif.). The p38 MAP kinase assay kits and SAPK/JNK assay kits were purchased from Cell Signaling (Beverly, Mass.). Immobilon-P transfer membranes used for Western blotting were obtained from Millipore (Bedford, Mass.). Dithiothreitol (DTT), β-glycerol phosphate, leupeptin, phenylmethylsulfonyl fluoride (PMSF), and sodium orthovanadate were obtained from Sigma Chemical (St. Louis, Mo.). The p38 inhibitor SB202190 was obtained from Calbiochem (La Jolla, Calif.).

Production of wild-type and mutant Shiga toxins. Wild-type Stx1 was prepared by receptor analog affinity chromatography (1). To heat inactivate the toxin, an aliquot of active reconstituted toxin was set aside and a paired sample was inactivated by boiling in a water bath for 8 h. Boiled toxin was checked for biological activity and did not inhibit [^{3}H]leucine incorporation in HCT-8 cells (25). A strain that produced a catalytic mutant Stx1 with a substitution of aspartic acid for glutamic acid at residue 167 in the active site was the kind gift of Matthew Jackson. For preparation of this mutant Stx1 (Stx1E167D), overnight cultures grown in Luria-Bertani broth plus ampicillin were harvested by centrifugation and then resuspended in 10 mM phosphate-buffered saline (PBS; pH 7.5) plus aprotinin (200 ng/ml) and 2 mM PMSF. The bacteria were lysed by passage through a French pressure cell (two passes at 24,000 lb/in^2; Spectronics, Urbana, Ill.). The lysate was cleared by centrifugation at 38,000 × *g* for 30 min. The supernatant was treated by ammonium sulfate precipitation; crude toxin was harvested from the 30-to-60% cut. After extensive dialysis in PBS, the crude toxin was purified by receptor analog affinity chromatography (1). Stx1E167D stocks were made by diluting lyophilized Stx1E167D in cell culture medium at 100 μg/ml. Stx1E167D was assayed by [^{3}H]leucine incorporation in Vero cells as previously described (16) and was approximately 500-fold less active than wild-type Stx1, consistent with previously reported data (12).

Confocal microscopy of HCT-8 cell uptake and trafficking of Stx1 and Stx1E167D. Purified Stx1 and Stx1E167D were directly labeled with Oregon Green and Texas Red according to the manufacturer's instructions (Molecular Probes, Eugene, Oreg.). The concentration of labeled toxins was then assessed by sodium dodecyl sulfate-polyacrylamide gel electrophoresis (SDS-PAGE) and Coomassie blue staining. Stx1 labeled with Oregon Green 488 or Texas Red in this manner retains biologic activity (B. P. Hurley and D. W. K. Acheson, unpublished results). Coverslips were precoated with rat tail collagen and placed in six-well plates, and 300 μl containing approximately 600,000 cells was used to seed the coverslips. Cells were allowed to adhere overnight and then exposed to fresh media containing 1 μg each of Stx1-Oregon Green and Stx1E167D-Texas Red/ml. At various times up to 4 h, coverslips were removed from media, washed, fixed in 4% glutaraldehyde, washed, incubated in 50 mM NH_4Cl, washed, and mounted in Vectorshield mounting medium (Vector, Burlingame, Calif.). Images were obtained using a Leica SP2 point-scanning confocal microscope equipped with a Leica 40× 1.25 HCX PL Apo lens (Leica Microsystems, Heidelberg, Germany). Oregon Green was excited using the 488-nm line of an argon laser (Melles Griot, Carlsbad, Calif.), with detection of emitted light set from 500 to 600 nm; Texas Red was excited using the 568-nm line of a krypton laser (Melles Griot), with detection from 580 to 680 nm. The sample was scanned sequentially with one excitation source at a time to minimize bleedthrough from the green channel to the red channel. The image overlay is done by the Leica software; the color values of the pixels in the red and green images are merged using a Boolean "or" operation done bit-by-bit between the two images and then displayed in the overlay image.

RNA isolation and Northern blotting. Following cell treatments, cells were disrupted using Qiagen shredders and total RNA was prepared using RNA binding columns according to the manufacturer's instructions (Qiagen Inc.). For

Northern blotting, 10 to 30 μg of total RNA was separated on glyoxyl agarose gels and transferred to nylon membranes according to the manufacturer's instructions (Ambion). IL-8, c-Jun, and glyceraldehyde-3-phosphate dehydrogenase (GAPDH) probes were used as previously described (25). The c-Fos probe was used as described by Cochran et al. (7). DNA probes were synthesized by random priming and labeled with [α-^{32}P]dCTP. The blots were hybridized overnight at 65°C, washed, and detected using phosphate-based hybridization and wash solutions (6).

Preparation of cell extracts for Western blotting and immunoprecipitation (IP) kinase assays. Following treatment and removal of cell culture media, cell culture plates were transferred to ice and the cells were washed twice with cold PBS and then scraped into cold PBS to which 10 μg of leupeptin/ml, 1 mM PMSF, and 0.5 mM DTT were added. Cells were pelleted by centrifugation at 4°C, the supernatant was removed, and pelleted cells were resuspended in Triton lysis buffer, consisting of 25 mM HEPES (pH 7.5), 300 mM NaCl, 1.5 mM $MgCl_2$, 2 mM EDTA (pH 8.0), 0.05% Triton X-100, 0.1 mM Na_3VO_4, 20 mM β-glycerol phosphate, 10 μg of leupeptin/ml, 1 mM PMSF, and 0.5 mM DTT. The resuspended cells were gently rocked at 4°C for 30 min; cellular debris was removed by centrifugation at 4°C. The supernatants were collected and frozen at −80°C. The concentrations of the cell extracts were determined using Bio-Rad protein assay reagent according to the manufacturer's instructions (Bio-Rad).

Western blotting for cleaved caspase 3. Cell extracts were separated by SDS-PAGE and then transferred to Immobilon-P (Millipore). After blocking, membranes were incubated with anti-cleaved caspase 3 antibody according to the manufacturer's instructions. Briefly, anti-cleaved caspase antibody was used at a 1:1,000 dilution and incubated with membranes at 4°C overnight with gentle rocking. Membranes were then washed, incubated with anti-rabbit immunoglobulin G coupled to horseradish peroxidase, washed, incubated with substrate, and exposed to film.

Protein kinase assays. All protein kinase assays were performed on cell extracts of equal protein concentrations. p38 kinase activity was assessed using the P38 MAP kinase assay kit from Cell Signaling according to the manufacturer's instructions. Briefly, 200 μg of protein extract was mixed with monoclonal antibody specific for phosphorylated p38 (Thr180/Tyr182) immobilized on Sepharose beads. These mixtures were incubated overnight at 4°C with gentle rocking. Immunoprecipitates were washed twice with the lysis buffer supplied in the kit, to which 1 mM PMSF had been added, and then washed with the kinase buffer supplied in the kit. Immunoprecipitates were then resuspended in 50 μl of kinase buffer that was supplemented with 200 μM ATP and 2 μg of ATF-2 fusion protein. Kinase reaction mixtures were incubated for 30 min at 30°C, and then the reaction was terminated with SDS-PAGE sample buffer, followed by analysis by SDS-PAGE and Western blotting using antibody specific for ATF-2 phosphorylated at Thr 71.

SAPK/JNK activity was assessed using the SAPK/JNK assay kit from Cell Signaling according to the manufacturer's instructions. Procedures were similar to that outlined for p38 activity above, except JNK/SAPK was precipitated from 250 μg of cell extract by adding c-Jun fusion protein immobilized on Sepharose beads. Kinase reactions were performed, and Western blotting was performed using antibody specific for Jun phosphorylated at Ser 63. Jun fusion protein substrate can undergo phosphorylation at Ser 63 and/or Ser 63 and Ser 73, yielding two bands of 33 and 35 kDa, respectively.

Cell viability assays. HCT-8 cells were plated in 96-well plates as previously described (25) and were allowed to attach overnight. Cells were then exposed to Stx1, heat-inactivated Stx1, or Stx1E167D, with or without the p38 inhibitor SB202190 at 48 μM. After incubation for various times, cell viability was assayed by detection of formazan dye following reduction of 3-(4,5-dimethylthiazol-2-yl)-2,5,-diphenyl tetrazolium bromide (MTT) by mitochondrial succinate dehydrogenase as previously described (4). Briefly, cells were washed with PBS, 200 ml of PBS (pH 7.2) containing 0.5 mg of MTT/ml was added to each well, and cells were incubated at 37°C for 1 h, washed with PBS, and solubilized with isopropanol. Formazan product was measured by determining absorbance at 540 nm, using a microplate reader.

Internucleosomal DNA fragmentation assays. HCT-8 cells were plated in six-well plates and were allowed to adhere overnight, washed to remove unadherent cells, and then exposed to treatments as above. At various times after treatments, supernatants were harvested and cells floating in the supernatants were collected by centrifugation. Both adherent and floating cells were then lysed separately, and the lysate from each was loaded on a spin column, washed, and eluted according to the manufacturer's instructions (Apoptotic DNA-ladder kit; Roche Diagnostics Corporation, Indianapolis, Ind.). The eluent was treated with RNase I, ethanol precipitated, resuspended in a small volume of Tris-EDTA solution, and then separated by agarose gel electrophoresis.

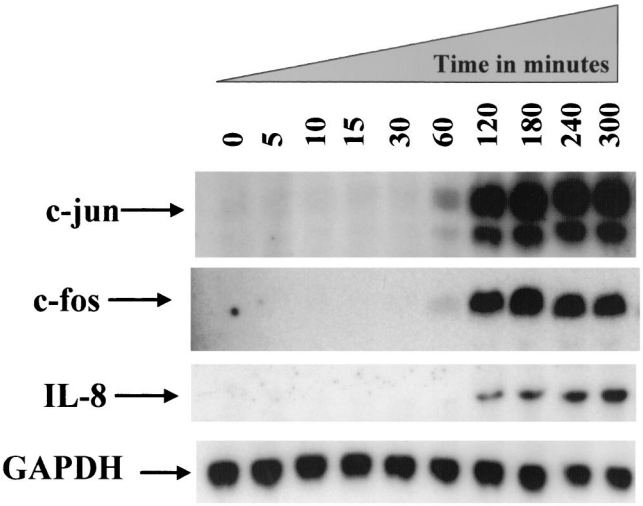

FIG. 1. Stx1 induces c-Jun, c-Fos, and IL-8 mRNA. At various times from 0 to 5 h after exposure to Stx1 (1 μg/ml), total RNA was harvested and a Northern blot was prepared from these samples and probed for c-Jun, c-Fos, IL-8, and GAPDH mRNA, as described in Materials and Methods. The time in minutes of RNA harvest is shown above each lane.

RESULTS

Induction of c-Jun and c-Fos mRNA by Stx1 occurs by 1 h. Previous data showed that Stxs can induce c-Jun and IL-8 mRNA and that heat-inactivated Shiga toxins are unable to induce these responses (25). Here, we focused on the timing of c-Jun, c-Fos, and IL-8 mRNA induction by Stx1. HCT-8 cells were exposed to Stx1 at 1 μg/ml; total RNA was isolated at times ranging from 0 to 300 min (5 h). A Northern blot was prepared and probed for c-Jun, c-Fos, and IL-8 mRNA, as shown in Fig. 1.

Figure 1 shows that induction of c-Jun mRNA by Stx1 is not detectable until 60 min after exposure to Stx1. Similar data were observed for c-Fos mRNA. These data clarified the time frame for MAP kinase activation in response to Stx1, which we hypothesized would occur before c-Jun, c-Fos, and IL-8 induction.

Shiga toxins activate p38 and JNK; this activation is dependent on Shiga toxin *N*-glycosidase activity. We next assessed the activation of the MAP kinases p38 and JNK in response to Stx1. Initially, we incubated HCT-8 cells with Stx1, heat-inactivated Stx1, or anisomycin (as a positive control) for times ranging from 0 to 60 min, harvested cell lysates, and measured p38 and JNK activity. Figure 2A shows that p38 activation in response to Stx1 is detectable 60 min after exposure, in contrast to the response to anisomycin, which occurs within 5 min. Heat-inactivated Stx1 did not result in significant p38 activation. Figure 2B shows that, as with p38 activation, JNK activation in response to Stx1 is detectable by 60 min after exposure, resulting in monophosphorylation of JUN substrate, whereas anisomycin activates JNK much more rapidly and strongly.

Because heat inactivation denatures the toxin protein, the failure of heat-inactivated toxin to activate MAP kinases does not rule out a Shiga toxin-associated activity distinct from its

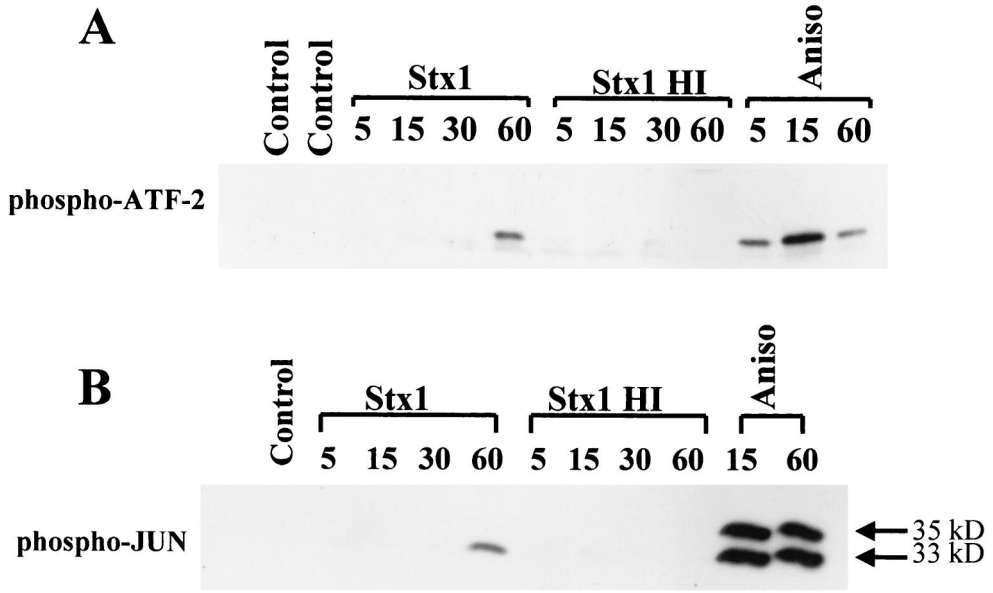

FIG. 2. Effect of Stx1 on p38 and JNK activation. At various times ranging from 5 to 60 min after exposure to Stx1 (1 μg/ml), heat-inactivated Stx1 (1 μg/ml), or anisomycin (1 μg/ml), whole-cell extracts were prepared, total protein was determined, and equal amounts of each extract were used to perform an IP kinase reaction for p38 (A) or for JNKs (B), as described in Materials and Methods. Note that anisomycin activates JNK more strongly than Stx1, resulting in phosphorylation of JUN substrate at both Ser 63 and Ser 73, yielding two bands of 33 kDa (monophosphorylated at Ser 63) and 35 kDa (phosphorylated at both Ser 63 and Ser 73). The time of whole-cell extract harvest is shown above each lane in minutes. Stx1 HI = heat-inactivated Stx1; Aniso = anisomycin.

enzymatic activity. In order to confirm that the *N*-glycosidase activity is responsible for MAP kinase activation, we used a toxin with a substitution mutation in the active site (E167D) that renders the mutant toxin approximately 500-fold less enzymatically active than wild-type Stx1 (data not shown). Before examining the effect of Stx1E167D on MAP kinase activation, we confirmed that the cellular uptake and trafficking of the mutant toxin in HCT-8 cells did not differ from that of wild-type Stx1. HCT-8 cells were plated on collagen-coated coverslips as described in Materials and Methods and incubated for 4 h with Stx1-Oregon Green 488 and Stx1E167D-Texas Red, each at a concentration of 1 μg/ml. Figure 3A shows the Stx1-Oregon Green 488 signal, Fig. 3B shows the Stx1E167D-Texas Red signal, and Fig. 3C shows the overlay images from Fig. 3A and B, demonstrating that the uptake and trafficking of Stx1-Oregon Green and Stx1E167D-Texas Red overlap completely in HCT-8 cells.

To assess the contribution of Stx1 enzymatic activity to MAP kinase activation, p38 and JNK activation levels were measured in lysates of cells exposed to native toxin or mutant toxin for the times shown in Fig. 4. Figure 4A shows that Stx1-induced p38 activation persists until at least 6 h after treatment; in contrast, the Stx1 E167D active-site mutant does not significantly induce p38. Similarly, Fig. 4B shows that while

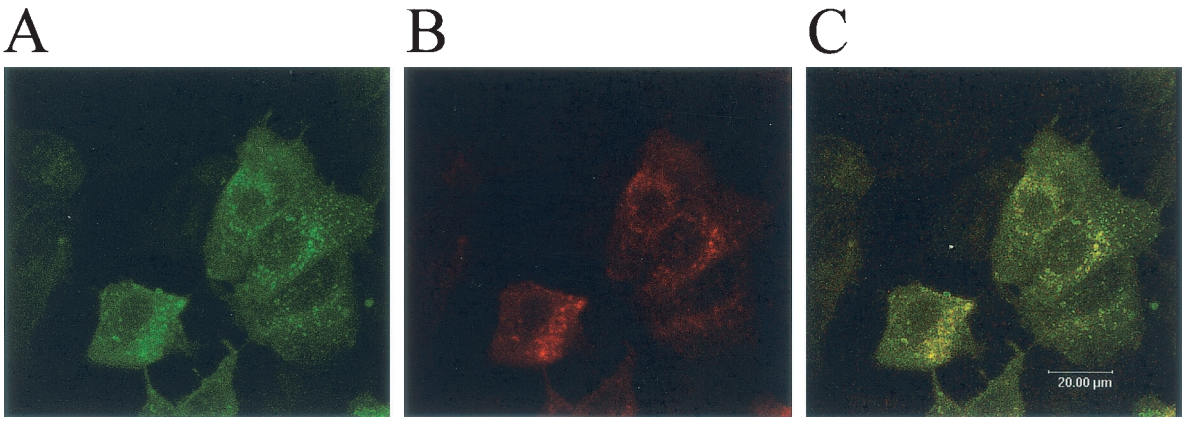

FIG. 3. Uptake and trafficking of Stx1-Oregon Green and Stx1E167D-Texas Red overlap completely in HCT-8 cells. HCT-8 cells were plated as described in Materials and Methods on collagen-coated coverslips and incubated for 4 h with Stx1-Oregon Green 488 and Stx1E167D-Texas Red, each at 1 μg/ml. Cells were then fixed and assessed by confocal microscopy as described in Materials and Methods. (A) Stx1-Oregon Green 488 signal; (B) Stx1E167D-Texas Red signal; (C) image overlay of panels A and B.

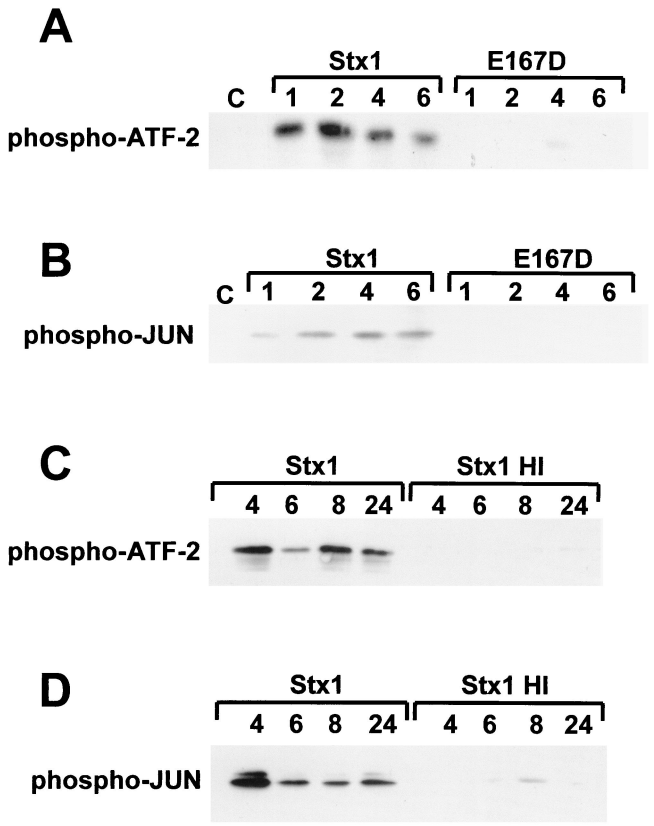

FIG. 4. Effect of Stx1 *N*-glycosidase mutant on p38 and JNK activation and duration of p38 and JNK activation in response to Stx1. (A and B) At various times ranging from 1 to 6 h after exposure to Stx1 (1 μg/ml) or mutant Stx1E167D (1 μg/ml), whole-cell extracts were prepared, total protein was determined, and equal amounts of each extract were used to perform an IP kinase reaction for p38 (A) or for JNKs (B), as described in Materials and Methods. The time of whole-cell extract harvest is shown above each lane in hours. E167D = mutant Stx1 with replacement of glutamic acid 167 with aspartic acid. (C and D) At various times ranging from 4 to 24 h after exposure to Stx1 (1 μg/ml) or heat-inactivated Stx1 (1 μg/ml), whole-cell extracts were prepared, total protein was determined, and equal amounts of each extract were used to perform an IP kinase reaction for p38 (C) or for JNKs (D), as described in Materials and Methods. The time of whole-cell extract harvest is shown above each lane in hours.

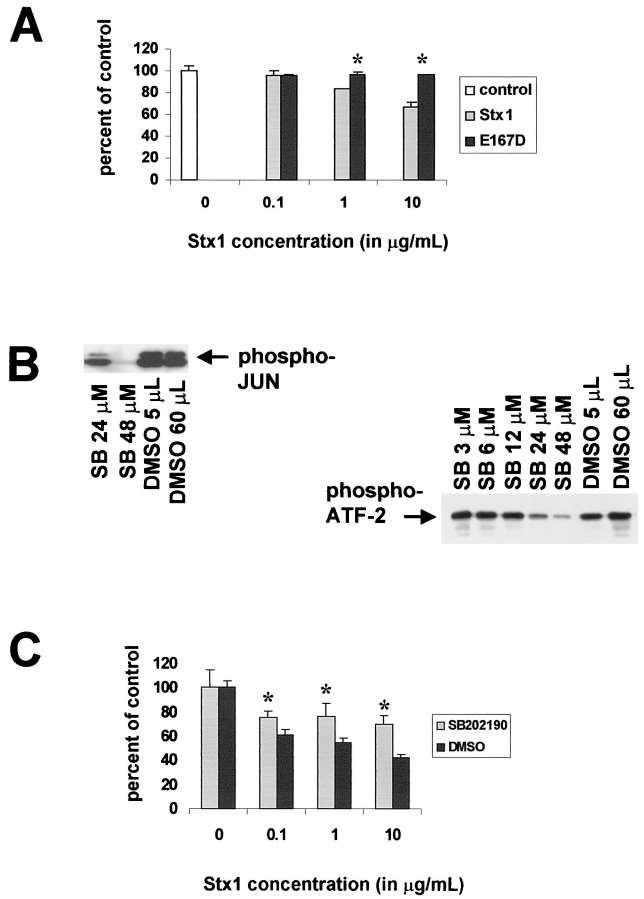

FIG. 5. Effect of SB202190 on Stx1-induced cell death and Stx1-induced p38 and JNK activation. (A) After treatment of HCT-8 cells for 72 h with various concentrations of Stx1 or Stx1E167D, cell viability was measured by MTT assay expressed as percentage of control cell viability. (B) Effects of various doses of SB202190 on Stx1-induced p38 and JNK activation in HCT-8 cells. Briefly, cells were preincubated with doses of SB202190 ranging from 3 to 48 μM, or equal amounts of the SB202190 diluent DMSO, and then exposed to Stx1 at 1 μg/ml. Cell extracts were obtained and assessments of p38 and JNK activation were performed as outlined in Materials and Methods. (C) After treatment of HCT-8 cells for 48 h with various concentrations of Stx1 with and without the p38 inhibitor SB202190, cell viability was measured by MTT assay and expressed as percentage of control cell viability. In panels A and C, optical density measurements for control cells were averaged, and then the optical density (at 540 nm) reading for each well in the microtiter plate was expressed as a percentage of the control average, including the individual control measurements. The percentages were then averaged for each group, and data are expressed as a mean ± standard deviation. For each condition, $n = 3$ wells. In panels A and C, * denotes a P value of <0.05 compared with control average.

Stx1-induced JNK activation persists until at least 6 h after treatment, the mutant toxin does not significantly induce JNK. Extension of the time frame showed that both p38 and JNK activation in response to Stx1 continued as long as 24 h (Fig. 4C and D). Again, heat-inactivated Stx1 did not significantly induce p38 or JNK activation compared to active Stx1.

Stx1 is cytotoxic in HCT-8 cells at high doses, and cytotoxicity can be blocked by the p38 inhibitor SB202190. Because p38 and JNK activation levels are prolonged in Stx1-treated HCT-8 cells, we assessed the fate of Stx1-treated HCT-8 cells over time, using the MTT assay to determine cell viability following Shiga toxin treatment. Not surprisingly, cell viability was decreased in response to Stx1 after 48 to 72 h; Stx1-induced cell death increased with toxin dose, and cell viability was unaffected by treatment with the Stx1E167D mutant. Confirming our previous findings, Stx1E167D induction of IL-8 protein in these samples was diminished compared to that with the wild type (data not shown).

In order to determine the role of the stress-activated protein kinase pathways in cell death, we then attempted to block Stx1-induced cytotoxicity by using the p38 inhibitor SB202190. First, we established the dose-response effects of SB202190 on Stx1-induced p38 and JNK activation in this cell line (Fig. 5B). We chose an SB202190 concentration of 48 μM for subsequent experiments because, at this dose, both p38 and JNK activities

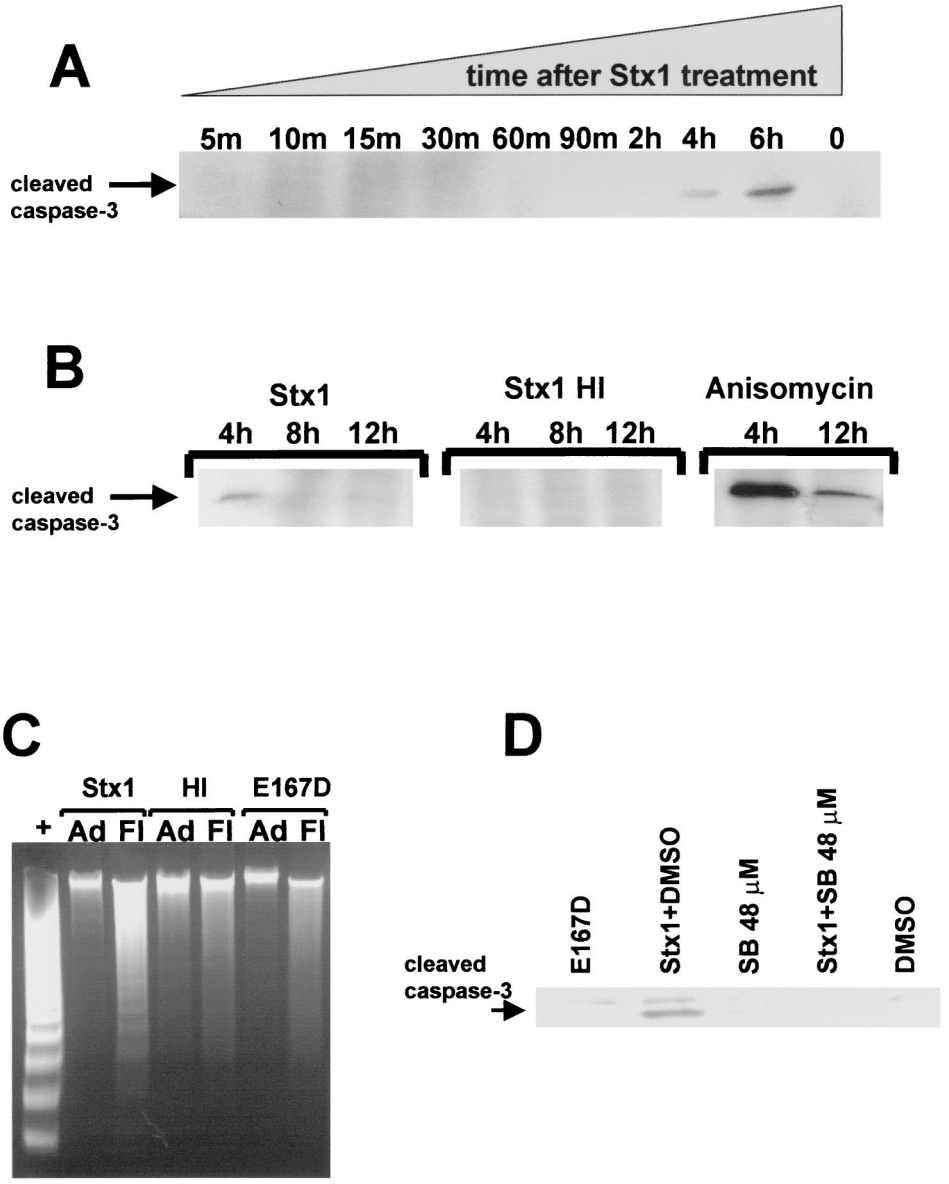

FIG. 6. Effect of Stx1 on caspase 3 cleavage and internucleosomal DNA fragmentation and effect of SB202190 on Stx1-induced caspase 3 cleavage. (A and B) Western blots for cleaved caspase 3. HCT-8 cells were incubated with Stx1 or heat-inactivated Stx1 at 1 μg/ml for the times noted above each lane. Cell extracts were prepared, protein concentrations were determined, and blots were prepared using 200 μg of each extract per lane. Anti-cleaved caspase 3 antibody was used to detect Stx1-induced caspase 3 cleavage, as described in Materials and Methods. In panel B, anisomycin was used at 1 μg/ml to treat HCT-8 cells as a positive control for caspase 3 cleavage. (C) Integrity of DNA extracted from either cells adherent to the plate (Ad) or cells floating in the culture supernatant (Fl) following treatment with Stx1, heat-inactivated Stx1 (Stx1 HI), or Stx1E167D (E167D) at a dose of 10 μg/ml for 22 h. +, positive control apoptotic cells provided in the kit. (D) Western blot for cleaved caspase 3. HCT-8 cells were preincubated with the inhibitor SB202190 at 48 mM for 30 min, or the SB202190 inhibitor diluent DMSO, and then exposed to Stx1 at 1 μg/ml for 4 h. HCT-8 cells incubated with SB202190 or DMSO are shown as negative controls. Cell extracts were obtained and used to perform Western blotting for cleaved caspase 3 as described above.

were significantly diminished. Figure 5C shows the effect of the p38 inhibitor SB202190 on HCT-8 cell viability after exposure to Stx1 for 48 h. In this experiment, cells were treated with Stx1 in the presence of the p38 inhibitor SB202190 or the SB202190 diluent dimethyl sulfoxide (DMSO). Control treatments consisted of no Stx1 treatment and exposure to SB202190 or DMSO alone. Use of the SB202190 inhibitor at this dose significantly protected HCT-8 cells from Stx1-induced cell death at all doses of Stx1 examined. Note that neither blockage nor rescue are complete. Use of SB202190 at 3 μM in the experiment shown in Fig. 5C did not prevent Stx1-induced cell death (data not shown).

Stx1 induces caspase 3 cleavage and DNA fragmentation in HCT-8 cells, and Stx1-induced caspase cleavage can be blocked by SB202190. Figure 6A and B show the results of Stx1 treatment on caspase 3 cleavage as detected by Western blot-

ting. Stx1 induces caspase 3 cleavage at 4 and 6 h; heat-inactivated Stx1 does not. In Fig. 6B, anisomycin-induced caspase 3 cleavage is shown as a positive control. We then assessed DNA integrity in HCT-8 cells following Stx1 treatment as a second indicator of apoptosis. Figure 6C shows the integrity of DNA extracted from either cells adherent to the plate or cells floating in the culture supernatant after treatment with Stx1, heat-inactivated Stx1, or the Stx1E167D mutant, all used at a concentration of 10 μg/ml for 22 h. DNA from adherent cells was intact after all cell treatments, as was DNA from cells floating in the culture supernatants after treatment with either heat-inactivated Stx1 or Stx1E167D. However, only DNA extracted from cells floating in the culture supernatant after treatment with Stx1 showed internucleosomal DNA fragmentation characteristic of apoptosis.

We attempted to block Stx1-induced caspase activation using high-dose SB202190, which prevented Stx1-induced cytotoxicity. Figure 6D shows the results of Stx1 treatment on caspase 3 cleavage in the presence and absence of SB202190. Stx1-induced caspase 3 cleavage is decreased by blocking p38 and JNK activation by using SB202190 at 48 μM. As also shown in Fig. 6D, treatment of cells with Stx1E167D does not induce caspase 3 cleavage.

DISCUSSION

Induction of c-Fos and c-Jun mRNA and activation of JNK following 28S rRNA damage defines the ribotoxic stress response, although the host signal transduction events linking 28S rRNA damage to activation of these MAP kinases are not known. Through ribotoxic stress, eukaryotic ribosomes may act as sensors of cellular damage and initiate changes in host cell functioning designed to respond to the specific stress encountered (24). In the present study, we have shown that Stx1 can activate the MAP kinase pathways JNK/SAPK and p38 in intestinal epithelial cells, the first host cells exposed to Shiga toxins during infection with STEC. Ribotoxic stress is the most likely mechanism by which this occurs, since Stx1 enzymatic activity was required for both JNK and p38 activation; a catalytically defective mutant toxin did not activate either of these MAP kinases. Consistent with the idea that Shiga toxins must first traffic to their site of enzymatic activity, Shiga toxin-induced p38 and JNK activity was first observed at 1 h after exposure, compared with much earlier activation observed with anisomycin, a relatively small compound (molecular weight, 265.3) that is thought to enter cells by diffusion. These data support the hypothesis that during STEC infection, intestinal epithelial cells are not simple gatekeepers modulating Shiga toxin traffic to deeper tissues but may also act as heralds of stress and participate in creating a gut milieu that favors immune activation of other cell types involved in HUS pathogenesis.

We also asked the question of what happens after ribotoxic stress is initiated in intestinal epithelial cells? To answer this question, the duration of Shiga toxin-induced p38 and JNK activation was assessed, and we observed persistent activation in these cells until the end of the assay at 24 h. We then evaluated cell viability after Shiga toxin treatment, and we observed cytotoxicity after 48 to 72 h that required Stx1 enzymatic activity. We observed that death occurred by apoptosis, based on assays for caspase 3 cleavage and internucleosomal DNA fragmentation. Stx1 enzymatic activity was required for both these markers of apoptosis. However, the long duration of p38 and JNK activation in response to Shiga toxins, followed by cellular apoptosis also linked to Stx1 enzymatic activity, suggested that the signal transduction events initiated by ribotoxic stress may result in the eventual apoptosis of these cells. To this end, we were able to block Stx1-induced cell death with an inhibitor of the p38 pathway used at a high dose (48 μM) in which JNK inhibition was also achieved. Furthermore, blocking p38 and JNK activity in this manner prevented Stx1-associated caspase 3 cleavage. To our knowledge, this is the first time that Stx1-induced p38 and/or JNK activation has been associated with Stx1-induced apoptosis. It is not simply Shiga toxin-associated protein synthesis blockade, but rather the specific activation of p38 and JNK resulting from the Shiga toxin-28S rRNA interaction that may promote apoptosis in intestinal epithelial cells.

In our experimental system, we were unable to find a dose of SB202190 that blocked p38 but not JNK activation, and we are thus unable to specify whether Stx1-induced p38 activation alone, JNK activation alone, or both, contribute to apoptosis. We propose in the future to use more specific inhibitors of p38 and JNK as well as dominant-negative constructs of these MAP kinases to answer this question.

Both p38 and JNK activation have previously been associated with cellular apoptosis in other cell lines with other stimuli (reviewed in reference 8), although their role is somewhat controversial because the requirement for JNK activation varies with experimental system (references 8 and 24 and references therein). Shifrin and Anderson used a variety of trichothecene toxins isolated from *Fusarium* species to assess the effects of peptidyltransferase inhibitors on p38/JNK activation and apoptosis. While many of these agents could strongly induce p38/JNK activation, induction of apoptosis occurred most strongly with agents that also caused translational arrest. Parallel to these findings, in the present study the doses of Stx1 used resulted in translational arrest. Interestingly, Shiga toxins have been evaluated for a potential therapeutic role as inducers of apoptosis in cancer cells. However, linking Shiga toxin with both cytokine expression and apoptosis in the same cell line raises a concern that, prior to cell death, Shiga toxins may stimulate an inflammatory response that could be detrimental to the host.

In addition to the damage caused by inflammation, the barrier function of the gut mucosa can be threatened by death of cells comprising that barrier. Recently, it has been hypothesized that Stx-induced apoptosis of gut epithelium could result in compromise of epithelial barrier function (5). Our data show that intestinal epithelial cells can be rescued from Shiga toxin-induced apoptosis by inhibiting p38 and/or JNK activation. Combined with our previous observations showing that Shiga toxin-induced IL-8 expression in intestinal epithelial cells can be decreased by inhibiting the p38 pathway (25), the present study suggests that blocking specific host signal transduction pathways in the gut may be a means by which both Shiga toxin-induced host immune activation, as well as Shiga toxin-induced apoptosis, can be diminished.

Some researchers have reported Shiga toxin holotoxins acting as proinflammatory stimuli in various experimental sys-

tems; others have reported these holotoxins acting as proapoptotic agents. Our observations suggest that the link between these two apparently distinct activities, at least for Shiga toxin holotoxin, may be in the induction of host stress-activated MAP kinases.

ACKNOWLEDGMENTS

Research support for this study included the following grants from the National Institutes of Health, Bethesda, Md.: A1-01715 (C.M.T.), AI-07389 (S.T.C.), and P30DK-34928 for the Center for Gastroenterology Research on Absorptive and Secretory Processes. C.M.T. was also supported by the Charles H. Hood Foundation.

We thank Bryan P. Hurley and Kinara S. Yang for technical assistance in using the fluorescently labeled Shiga toxins.

REFERENCES

1. **Acheson, D. W., M. Jacewicz, A. V. Kane, A. Donohue-Rolfe, and G. T. Keusch.** 1993. One step high yield affinity purification of Shiga-like toxin II variants and quantitation using enzyme linked immunosorbent assays. Microb. Pathog. **14:**57–66.
2. **Banatvala, N., P. M. Griffin, K. D. Greene, T. J. Barrett, W. F. Bibb, J. H. Green, J. G. Wells, and The Hemolytic Uremic Syndrome Study Collaborators.** 2001. The United States National Prospective Hemolytic Uremic Syndrome Study: microbiological, serological, clinical and epidemiological findings. J. Infect. Dis. **183:**1063–1070.
3. **Barnett-Foster, D., M. Abul-Milh, M. Huesca, and C. A. Lingwood.** 2000. Enterohemorrhagic *Escherichia coli* induces apoptosis which augments bacterial binding and phosphatidylethanolamine exposure on the plasma membrane outer leaflet. Infect. Immun. **68:**3108–3115.
4. **Berridge, M. V., and A. S. Tan.** 1993. Characterization of the cellular reduction of 3-(4,5-dimethylthiazol-2-yl)-2,5-diphenyltetrazolium bromide (MTT): subcellular localization, substrate dependence, and involvement of mitochondrial electron transport in MTT reduction. Arch. Biochem. Biophys. **303:**474–482.
5. **Ching, J. C. Y., N. L. Jones, P. J. M. Ceponis, M. A. Karmali, and P. M. Sherman.** 2002. *Escherichia coli* Shiga-like toxins induce apoptosis and cleavage of poly(ADP-ribose) polymerase via in vitro activation of caspases. Infect. Immun. **70:**4669–4677.
6. **Church, G. M., and W. Gilbert.** 1984. Genomic sequencing. Proc. Natl. Acad. Sci. USA **81:**1991–1995.
7. **Cochran, B. H., J. Zullo, I. M. Verma, and C. D. Stiles.** 1984. Expression of the c-fos gene and of a fos-related gene is stimulated by platelet-derived growth factor. Science **226:**1080–1082.
8. **Cross, T. G., D. Scheel-Toellner, N. V. Henriquez, E. Deacon, M. Salmon, and J. M. Lord.** 2000. Serine/threonine protein kinases and apoptosis. Exp. Cell Res. **256:**34–41.
9. **Foster, G. H., C. S. Armstrong, R. Sakiri, and V. L. Tesh.** 2000. Shiga toxin-induced tumor necrosis factor alpha expression: requirement for toxin enzymatic activity and monocyte protein kinase C and protein tyrosine kinases. Infect. Immun. **68:**5183–5189.
10. **Griffin, P. M., L. D. Olmstead, and R. E. Petras.** 1990. *Escherichia coli* O157:H7-associated colitis. Gastroenterology **99:**142–149.
11. **Heyderman, R. S., M. Soriani, and T. R. Hirst.** 2001. Is immune cell activation the missing link in the pathogenesis of post-diarrhoeal HUS? Trends Microbiol. **9:**262–266.
12. **Hovde, C. J., S. B. Calderwood, J. J. Mekalanos, and R. J. Collier.** 1988. Evidence that glutamic acid 167 is an active-site residue of Shiga-like toxin I. Proc. Natl. Acad. Sci. USA **85:**2568–2572.
13. **Hurley, B. P., C. M. Thorpe, and D. W. K. Acheson.** 2001. Shiga toxin translocation across intestinal epithelial cells is enhanced by neutrophil transmigration. Infect. Immun. **69:**6140–6147.
14. **Ikeda, M., Y. Gunji, S. Yamasaki, and Y. Takeda.** 2000. Shiga toxin activates p38 MAP kinase through cellular Ca^{2+} increase in Vero cells. FEBS Lett. **485:**94–98.
15. **Iordanov, M., M. D. Pribnow, J. L. Magun, et al.** 1997. Ribotoxic stress response: activation of the stress-activated protein kinase JNK1 by inhibitors of the peptidyl transferase reaction and by sequence-specific damage to the α-sarcin/ricin loop in the 28S rRNA. Mol. Cell. Biol. **17:**3373–3381.
16. **Jacewicz, M., H. A. Feldman, A. Donohue-Rolfe, K. A. Balasubramanian, and G. T. Keusch.** 1989. Pathogenesis of Shigella diarrhea. XIV. Analysis of Shiga toxin receptors on cloned HeLa cells. J. Infect. Dis. **159:**881–889.
17. **Jones, N. L., A. Islur, R. Haq, M. Mascarenhas, M. A. Karmali, M. H. Perdue, B. W. Zanke, and P. M. Sherman.** 2000. *Escherichia coli* Shiga toxins induce apoptosis in epithelial cells that is regulated by the Bcl-2 family. Am. J. Physiol. Gastrointest. Liver Physiol. **278:**G811–G819.
18. **Keenan, K. P., D. D. Sharpnack, H. Collins, S. B. Formal, and A. D. O'Brien.** 1986. Morphologic evaluation of the effects of Shiga toxin and *E. coli* Shiga-like toxin on the rabbit intestine. Am. J. Pathol. **125:**69–80.
19. **Kyriakis, J. M., and J. Avruch.** 2001. Mammalian mitogen activated protein kinase signal transduction pathways activated by stress and inflammation. Physiol. Rev. **81:**807–869.
20. **Nakamura, A., E. J. Johns, A. Imaizumi, Y. Yanagawa, and T. Kohsaka.** 2001. Activation of β_2-adrenoceptor prevents Shiga toxin-2 induced TNF-α gene transcription. J. Am. Soc. Nephrol. **12:**2288–2299.
21. **Nash, S., J. Stafford, and J. L. Madara.** 1987. Effects of polymorphonuclear leukocyte transmigration on barrier function of cultured intestinal epithelial monolayers. J. Clin. Investig. **10:**1104–1113.
22. **Parsons, P. E., K. Sugahara, G. R. Cott, R. J. Mason, and P. M. Henson.** 1987. The effect of neutrophil migration and prolonged neutrophil contact on epithelial permeability. Am. J. Pathol. **129:**302–312.
23. **Paton, J. C., and A. W. Paton.** 1998. Pathogenesis and diagnosis of Shiga toxin-producing *Escherichia coli* infections. Clin. Microbiol. Rev. **11:**450–479.
24. **Shifrin, V. I., and P. Anderson.** 1999. Tricothecene mycotoxins trigger a ribotoxic stress response that activates c-Jun N-terminal kinase and p38 mitogen-activated protein kinase and induces apoptosis. J. Biol. Chem. **274:**13985–13992.
25. **Thorpe, C. M., B. P. Hurley, L. L. Lincicome, M. Jacewicz, G. T. Keusch, and D. W. K. Acheson.** 1999. Shiga toxins stimulate secretion of interleukin-8 from intestinal epithelial cells. Infect. Immun. **67:**5985–5993.
26. **Thorpe, C. M., W. E. Smith, B. P. Hurley, and D. W. K. Acheson.** 2001. Shiga toxins induce, superinduce, and stabilize a variety of C-X-C chemokine mRNA in intestinal epithelial cells resulting in increased chemokine expression. Infect. Immun. **69:**6148–6155.

Editor: A. D. O'Brien